Computational Models for Trapping Ebola Virus Using Engineered Bacteria

Daniel P. Martins, Michael Taynnan Barros, Massimiliano Pierobon, Meenakshisundaram Kandhavelu, Pietro Lio', and Sasitharan Balasubramaniam

Abstract—The outbreak of the Ebola virus in recent years has resulted in numerous research initiatives to seek new solutions to contain the virus. A number of approaches that have been investigated include new vaccines to boost the immune system. An alternative post-exposure treatment is presented in this paper. The proposed approach for clearing the Ebola virus can be developed through a microfluidic attenuator, which contains the engineered bacteria that traps Ebola flowing through the blood onto its membrane. The paper presents the analysis of the chemical binding force between the virus and a genetically engineered bacterium considering the opposing forces acting on the attachment point, including hydrodynamic tension and drag force. To test the efficacy of the technique, simulations of bacterial motility within a confined area to trap the virus were performed. More than 60 percent of the displaced virus could be collected within 15 minutes. While the proposed approach currently focuses on *in vitro* environments for trapping the virus, the system can be further developed into a future treatment system whereby blood can be cycled out of the body into a microfluidic device that contains the engineered bacteria to trap viruses.

Index Terms—Ebola virus, genetically engineered bacteria, microfluidic viral attenuator

1 Introduction

The recent outbreak of Ebola virus has resulted in concerns by the research community to develop new solutions that can curb and control its spreading process [1]. While the majority of Ebola virus outbreaks are currently found in Africa, their rate of spreading requires immediate attention. The spreading process of Ebola virus is through the exchange of fluids between individuals, animals, as well as within the environment where the virus lies. Poor sanitary conditions in the developing countries also fuel the spreading process, which has detrimental effects on lives and on the socio-economical stability of the affected regions.

Currently, there are preventive and post-exposure treatments available [2] [3]. Two vaccines were developed and are still being tested in Guinea: one developed by Merck Sharp and Dohme and another by Toyama Chemical [4], [5]. Other advanced research for solutions to the Ebola virus disease problem is in the domain of molecular biology and biotechnology [6]. Based on this, a number of therapeutic medications to treat Ebola virus disease has been developed and tested, and this includes TKM-Ebola, amiodarone, dronedarone, verapamil and ZMapp [3], [7], [8]. ZMapp is a cocktail of three monoclonal antibodies produced from Tobacco plants (*Nicotiana benthamiana* species) and provides immunity to the Ebola virus. Successful tests were made on mice and non-human primates [8], [9]. Also, monoclonal antibodies derived from a person who survived Ebola virus disease protected non-human primates when given as late as 5 days after the infection [10], [11]. Other treatments that have compounds capable of blocking Ebola virus-like particles from entry into the cells and a novel peptide vaccine have also been proposed to increase the range of available treatments [12], [13]. While the effectiveness of those vaccines for large scale population is still under investigation, another outbreak can occur. Therefore, we propose an alternative post-exposure treatment using synthetic biology to engineer bacteria that can trap the virus, and utilize this solution through a microfluidic attenuator.

The field of *synthetic biology* has received tremendous attention in recent years, due largely to the potential impact of delivering new solutions for biotechnology [6], [14]. Synthetic biology enables genetic circuits to be designed and inserted into cells in order to create new properties as well as functionalities. For example the field of *molecular communication* [15], [16] aims to construct bio-compatible communication systems based on programming of cells. Engineered bacteria through synthetic biology have also been used as therapeutic agents in the past [17]. For example, HIV-1

- *D.P. Martins and M.T. Barros are with the Telecommunication Software & Systems Group (TSSG), Waterford Institute of Technology (WIT), Waterford, X91 P20H, Ireland. E-mail: {dpmartins, mbarros}@tssg.org.*
- *M. Pierobon is with the Department of Computer Science and Engineering, University of Nebraska-Lincoln, Lincoln, NE 68588. E-mail: maxp@unl.edu.*
- *M. Kandhavelu is with the Department of Signal Processing, Tampere University of Technology, Tampere 33720, Finland. E-mail: meenakshisundaram.kandhavelu@tut.fi.*
- *P. Lio' is with the Computer Laboratory, University of Cambridge, Cambridge CB2 1TN, United Kingdom. E-mail: pl219@cam.ac.uk.*
- *S. Balasubramaniam is with the Telecommunication Software & Systems Group (TSSG), Waterford Institute of Technology (WIT), Waterford, Ireland, and the Nano Communications Center (NCC), Department of Electronics and Communication Engineering, Tampere University of Technology (TUT), Tampere 33720, Finland. E-mail: sasi.bala@tut.fi.*

Manuscript received 20 Nov. 2016; revised 29 Aug. 2017; accepted 23 Sept. 2017. Date of publication 15 May 2018; date of current version 6 Dec. 2018. (Corresponding author: Daniel P. Martins.)
For information on obtaining reprints of this article, please send e-mail to: reprints@ieee.org, and reference the Digital Object Identifier below.
Digital Object Identifier no. 10.1109/TCBB.2018.2836430

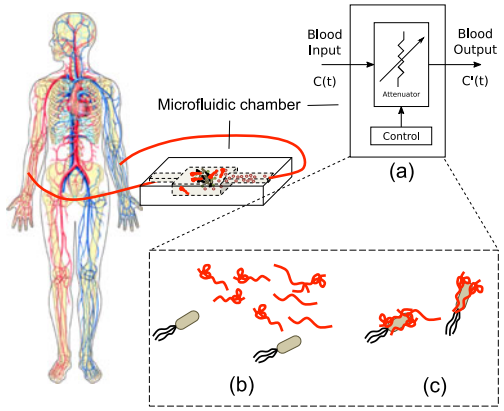

Fig. 1. Illustration of the proposed approach, where blood infected with Ebola is passed through an external tube with a microfluidic chamber containing genetically engineered bacteria that are used to trap the Ebola virus. (a) The microfluidic chamber is represented as an attenuator. (b) Bacteria move towards the Ebola virus scattered in the chamber. (c) Bacteria after trapping the virus onto their surface membrane.

infection in CD4+ T cells and macrophages were inhibited using *Lactobacillus jensenii* bacteria [17]. Bacteria have also been used to hunt down and eradicate human lymphomas [18].

In this paper, we propose synthetically engineered bacteria (*Escherichia coli*) that moves and traps Ebola virus in a sponge-like manner [19]. While our theoretical models and analysis presented in this paper are based on *in vitro* environments, the proposed approach has the potential to be used for designing future treatment systems as illustrated in Fig. 1. The blood contaminated with Ebola virus is transported through a cyclic external tube that goes through a microfluidic attenuator, and back into the body again. The engineered bacteria within the chamber will collide and trap the Ebola through the protein binding process on the surface membrane, resulting in the virus attachment. The proposed system can be described as

$$C'(t) = f_b(t)C, \tag{1}$$

where $C'(t)$ is the Ebola concentration in out-going blood flow, C is the incoming concentration of Ebola virus in the blood stream and $f_b(t)$ is the attenuation function described by the bacterial trapping performance.

The process of virus traping has been previously investigated. For example, in [19] red blood cells are used to trap viruses. These cells are ideal for virus trapping due to the fact that they lose their nuclei as they mature. Therefore, when the virus infects the red blood cell, it will have no capability of replicating itself due to the missing DNA, and hence, leading to a trapping process. Another example is in [20], where the authors specifically studied the *Phi-6* virus, which typically invades *Pseudomonas phaseolica*. This particular bacterium attaches itself to the plants by using its hair like structure that extends from their body. The attachment is achieved when the bacterium contracts its body enabling the thick hair to grip onto the surface of the plant. In order to trap the virus, the authors engineered the bacteria to have excessive amount of hair on the surface leading to minimal amount of space to allow the virus to penetrate through the membrane but enough to embed and get stuck on the microbes [20].

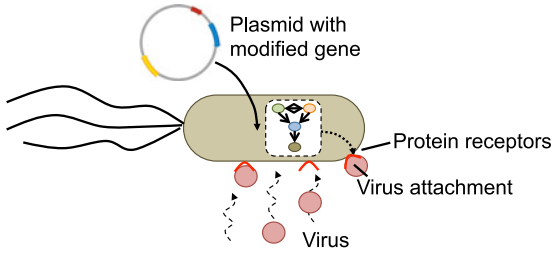

Fig. 2. Genetically engineered bacteria will produce proteins on the surface that will allow the virus to bind.

The most common mechanism for virus binding on the cell's surface is through the polyvalent interactions between the proteins and the cell's receptors [21]. This process is similar to what we are proposing in this paper. However, there are a number of challenges to be addressed. First, a compatible binding process is required between the virus and the bacterium. The compatible receptors on the bacterium can be engineered through synthetic biology as illustrated in Fig. 2, where genes that are inserted into the plasmid can lead to expression of proteins on the surface. Second, Ebola virus has a long filamentous structure unlike other types of virus, and usually with a higher molecular weight. Therefore, the binding process may not cover the entire length of the virus, leading to parts of the virus hanging from the bacterium after binding. This means that the binding process must be strong enough to support the momentum of the hanging virus body, in particular when faced with hydrodynamic tension and drag.

The contributions of this paper include:

- **A design of Ebola virus microfluidic attenuator system** based on a cleaning process, where the bacteria are used to collect and trap the Ebola virus. This trapping process will minimize the virus concentration in blood to curb them from replicating and spreading.
- **A binding force model** to trap Ebola virus in free moving bacteria, considering their swimming and tumbling process, as well as opposing forces resulting from the hydrodynamic tension and drag and the weight of the hanging body of the virus.
- **A simulation of bacteria motility process** is developed to evaluate the effectiveness of trapping an Ebola virus population in a confined area.

The paper is organized as follows. Section 2 describes the physical properties of Ebola virus. The engineering of proteins on the bacteria surface to bind to the virus is presented in Section 3. Section 4 describes the binding force models between the bacteria and the virus. The simulation evaluation and results are presented and discussed in Section 5. Lastly, Section 6 presents the conclusion.

2 Background on Ebola Virus

Ebola virus belongs to the order *Mononegavirales* from the *Filoviridae* family. Upon infection, it can kill up to 50 percent of the patients within 6 to 16 days [22]. The virus has

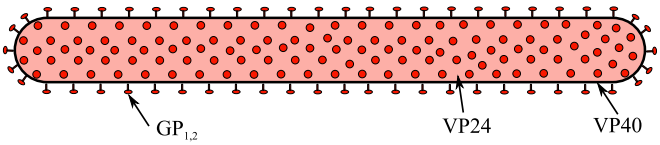

Fig. 3. Structure of an Ebola virus, including the membrane-spanning protein ($GP_{1,2}$) and the proteins that build the inner matrix (VP40 and VP24).

a filamentous shape, with a uniform width of nearly 80 nm and a length of approximately 970 nm, and its structure is illustrated in Fig. 3. According to this structure, the virus membrane consists of $GP_{1,2}$ (spike glycoprotein) and two other proteins, VP40 and VP24 (primary and secondary matrix proteins). $GP_{1,2}$ is a membrane-spanning protein, and VP40 and VP24 builds the inner matrix [23], [24]. The glycoproteins are 7 nm in diameter and have a spacing of 10 nm between each other. The glycoproteins enable the Ebola virus to bind and submerge itself into the host cells (process required for viral internalization) [23].

There are three infection routes for the Ebola virus: through mucosal surfaces (mouth, eyes, genitalia), skin abrasions or through the use of contaminated needles [24]. After the virus enters the body, it spreads rapidly [24], [25], [26], [27], and is capable of overcoming responses from the immune system. The high rate of virus replication inside the immune system cells hinders the human body defenses [25], [26], [27]. Monocytes, macrophages and dendritic cells are the front door for the Ebola virus infection, and preferred sites of replication [26]. In addition, these cells are used as vehicles to spread the Ebola virus through the lymphatic system [24]. Infected monocytes and macrophages secrete soluble factors to recruit other similar cells inside the lymph nodes to increase the infection. In latter stages, hepatocytes and adrenal cortical cells are infected and the production of coagulation factors is decreased, which results in internal bleeding [28].

3 Engineering Protein Binding

3.1 Synthetic Protein Binding Receptors

The main challenge of lowering the concentration of the Ebola virus using bacteria lies in using synthetic biology to produce the required proteins on the surface membrane to bind the virus. In particular, careful understanding of viral entry and replication mechanisms into the host system is required before suitable genetic circuits can be developed. Past research have used dual color synthetic constructs to observe how a single virus affects the host bacterium and determine the level of infection [29]. Single-virus tracking methods have also been developed to observe the mode of interaction between *E. coli* and bacteriophage lambda [29]. In our proposed model, it is possible to construct a synthetic gene that could increase the expression of Ebola virus protein binding receptors. Facilitating the binding frequency between the viral proteins and over expressed membrane receptor proteins would be an advantage to harvest the target virus. Specifically, reports have suggested that the cell surface receptor *T-cell Immunoglobulin Mucin domain 1* (*TIM-1*) of epithelial cells favourably increases the binding of Ebola virus. A study on over expression of fluorescent tagged *TIM-3* protein in *E. coli* also confirms that TIM-like protein can have a functional property which allows viral protein recognition and binding [30]. Therefore, the TIM-like protein could be one of the possible targets to be expressed in *E. coli* to create engineered bacteria to trap the Ebola virus. Engineering the synthetic circuit of *EnvZ*/*OmpR*/*BolA* genes along with the TIM-like protein-coding genes will facilitate the binding of Ebola virus and simultaneously control the motility of *E.coli* during the binding and trapping of Ebola virus (*EnvZ* is the sensor-transmitter kinase that phosphorylates *OmpR*, a DNA-binding regulatory protein, under stress conditions) [31], [32]. Another requirement is the engineering of the bacteria to prevent the virus entry, and this could be achieved by considering the use of mutant *E.coli* as a host that carries membrane proteins (*e.g.*, Porins) [33], [34].

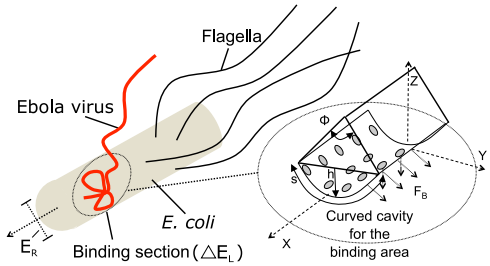

Fig. 4. Expanded view of the partial deformation on the bacterium surface membrane when the virus binds on its surface.

3.2 Protein Binding Model

Our model is developed as a function of the binding among bacterial receptors and the viral glycoproteins. We analyse the produced binding force, and how it will counter the opposing forces (due to drag and weight of the virus) that can result in the attachment breakage. During the binding process, the virus deforms the bacterium surface creating a curved cavity with a submergence angle ϕ (in radians) as shown in Fig. 4 [35]. The cavity segment consist of height h and arc length s. The attachment area B_{Area} between the virus and the bacterium can be evaluated as

$$\begin{aligned} B_{Area} &= s\Delta E_L \\ &= \phi E_R \Delta E_L, \end{aligned}$$

where E_R is the Ebola virus radius and ΔE_L is the length of the portion of Ebola virus that attaches to the bacterium. The reaction between the bacterial receptors and the virus proteins within B_{Area} can be represented as [35]:

$$\mathrm{n[V] + m[B]} \underset{\longleftarrow}{\overset{\mathrm{K_a}}{\longrightarrow}} \mathrm{[B_m V_n]}, \tag{2}$$

where n is the number of viral proteins that bind to a single bacterial receptor; m is the number of bacterial receptors that binds to a single viral protein; $[V]$ and $[B]$ are the concentrations of viral proteins and bacterial receptors, respectively; and K_a is the association binding constant for the reaction. The initial values for the viral and bacterial proteins ($[V_0]$ and $[B_0]$) are the ratio between the minimum attachment area and the area occupied by the Ebola glycoprotein and TIM-1, respectively. Therefore, the fraction p of the bacterial receptors that are bound by the viral proteins can be defined as [36]

$$p = \frac{\mathrm{[B_m V_n]}}{\mathrm{[V] + [B_m V_n]}}. \tag{3}$$

The total binding energy resulting from the complex formation of the Ebola virus glycoprotein and the bacterium receptors is represented as [37]:

$$E_{Total} = (E_{Bind} + (p-1)T_a S_0)B_{Area}, \tag{4}$$

where T_a is the absolute temperature; S_0 is the translational and rotational entropy of binding for this complex. The affinity binding energy E_{Bind} can be evaluated as follows:

$$E_{Bind} = -pk_B T_a \ln K_a, \tag{5}$$

where k_B is the Boltzmann constant. Based on the E_{Bind}, the binding force F_{Bind} for this process is represented as

$$F_{Bind} = -\frac{\partial E_{Total}}{\partial \phi}. \tag{6}$$

Since each virus will occupy a small area of the bacterium, the surface area can accommodate a number of Ebola virus. The limit for the number of virus that can bind to each bacterium b_{limit} can be represented as:

$$b_{limit} = bac_{Area} - \sum_{i=0} B^i_{Area}, \tag{7}$$

where bac_{Area} is the bacterium surface area and $i = 0, 1, 2, ...$ is the number of attached virus.

4 Force Model for Virus Detachment

In general, to achieve the stability of attachment, the binding force will highly depend on the opposing forces that include hydrodynamic drag force as well as the tensions exerted on the Ebola virus. The equilibrium will depend on B_{Area} and the motion realized by both bodies. After binding, both bodies can move in a straight line or tumble in a fixed location. For each movement, different tensions will affect the attachment. In this section, we discuss the tensions and forces that are exerted onto the virus during the bacterium's movement.

4.1 Hydrodynamic Drag Force

The medium that we consider is the blood, where the Ebola virus will diffuse through Brownian motion. Once the Ebola virus has attached itself to the bacterium, both are subjected to the same hydrodynamic force (drag force) as they mobilize. Since we model the shape of the bacterium as a cylinder, the $\mathbf{F_{Drag}}$ can be expressed as follows [38]:

$$\mathbf{F_{Drag}} = -\frac{1}{2}\rho_f v^2 A C_d, \tag{8}$$

where ρ_f is the fluid medium density, $v = v_b - v_f$ is the relative velocity between the bacterium (v_b) and the fluid (v_f), $A = \pi B_R^2$ is the bacterium's cross-section and B_R is the radius. The drag coefficient C_d is expressed as [38]:

$$C_d = \frac{24}{Re} + \frac{6}{1+\sqrt{Re}} + 0.4, \tag{9}$$

where the Reynolds number (Re) is expressed as [38]:

$$Re = \frac{D_v \rho_f v}{\eta_f}, \tag{10}$$

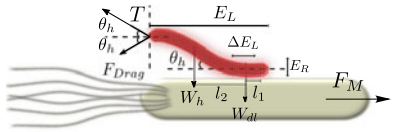

Fig. 5. The binding force representation model between an Ebola virus and the bacterium. The opposing tension force **T** is responsible for peeling the virus from the surface of the bacterium while the other forces act to maintain their attachment stability.

where η_f is the fluid viscosity, and D_v is the width of the microfluidic chamber.

4.2 Bacteria Motility

Bacteria have different types of motility (*e.g.*, swarming and swimming) [39]. When swimming, bacteria utilise their flagella to swim in a regular or biased motion towards a source (e.g., nutrients). Bacteria can also move in a coordinated manner across solid or semi-solid surfaces [39]. This motility process is known as swarming, and it is performed by group of cells instead of single individuals. This form of motility also depends on the *pili* formation that helps the cells to aggregate into a population [39]. For our model, we consider that the bacteria will swim and will not be allowed to grow or attach onto other surfaces, which is based on the swarming and gliding process. Also, our aim is to allow the bacteria the freedom of random movement to trap the Ebola virus, and this could be achieved through their swimming process.

The swimming process of the *E. coli* is based on their *flagella* movement. The flagella are tails that stem from the body of the *E. coli*. The swimming behavior of the bacteria is based on a cycle of run and tumble motion, and is governed by a random walk. During swimming, the flagella will wrap into a single body, and this will rotate as a propeller allowing them to swim forward. The bacteria swims in a straight line for an average period (λ_{Run}) that is based on an exponential distribution [40]. After swimming for a short period, the flagella will unwrap into individual strands and this will lead to tumbling in a fixed location. The average tumbling period is based on an exponential distribution (λ_{Tumble}) [40]. After the tumbling process, the bacterium will select a random angle to continue swimming. The binding between the bacterium and the virus will occur when they come into contact with each other.

4.3 Tension Force for Running Motion

The bacterium running motion (see Fig. 5) produces tension on the binding area that could break the attachment. In order to analyse the forces affecting the binding between two bodies, we use the approach presented in [41]. The description of each variable is as follows: ΔE_L is the length of the Ebola virus that binds to the bacterium surface (we are assuming here that only a portion of the virus has bound), $\mathbf{F_M}$ is the force exerted by the bacterium flagella that enable the movement, $\mathbf{W_h}$ is the weight for the hanging section of the Ebola virus, $\mathbf{W_{dl}}$ is the weight for the bound section of the Ebola virus, **T** is the tension exerted on the hanging portion of the Ebola virus that attempts to peel it from the bacterium due to resistance, l_1 is the distance between the bound mid-section of the Ebola virus and the bacterium centre of mass, l_2 is the distance between the centre of the Ebola virus hanging section and its bound mid-section, and θ_h is the angle between

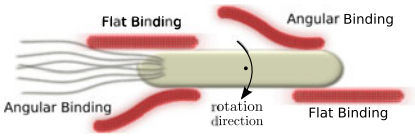

Fig. 6. Illustration of attachment points for angular and flat binding of the Ebola virus on the bacterium as it is going through a tumbling process. The positions of the flat and angular binding are dependent on the clockwise rotation of the bacterium.

the hanging portion of the virus and the bacterium. We consider both the Ebola virus and the bacterium as homogeneous bodies. Therefore,

$$\mathbf{W_{dl}} = \frac{m_e}{E_L} g \Delta E_L$$

and

$$\mathbf{W_h} = m_e g - \mathbf{W_{dl}} \ ,$$

where m_e is the Ebola virus mass and g is the gravitational constant. In order for the body to move linearly in a particular direction, the sum of the momenta has to be equal to zero. Therefore,

$$\sum M = M_{dl} + M_h + M_g + M_d - M_T = 0, \tag{11}$$

where $M_{dl} = \mathbf{W_{dL}} l_1$ is the momentum due to the force exerted on ΔE_L, $M_h = \mathbf{W_h}(l_2 + l_1)\cos\theta_h$ is the momentum due to the force exerted on the hanging section of the Ebola virus, $M_g = \int_0^{\Delta E_L} P_n \ x \ dx$ is the momentum due to the force exerted on the glycoprotein-receptor complexes on the bacterium (where P_n is the adhesive pressure of all the glycoproteins and x is the length of the Ebola virus binding area), $M_d = \mathbf{F_{Drag}} \sin\theta_h E_L$ is the momentum due to the drag force exerted on the edge of the Ebola virus ($\mathbf{F_{Drag}}$ is calculated from Eq. (8)), and $M_T = \mathbf{T} E_L \sin\theta_h$ is the momentum due to the tension exerted on the hanging section of the Ebola virus. By replacing these terms into Eq. (11) as well as the relationship of $l_2 = (\frac{E_L}{2} - \frac{\Delta E_L}{2})$, which is the distance between the weights $\mathbf{W_{dL}}$ and $\mathbf{W_h}$, the tension $\mathbf{T}$ can be represented as:

$$\begin{aligned}\mathbf{T} = \Bigg(& \mathbf{W_{dl}} l_1 + \mathbf{W_h}\left(\frac{E_L}{2} - \frac{\Delta E_L}{2} + l_1\right)\cos\theta_h \\ & + \frac{P \Delta E_L^2}{2} + \mathbf{F_{Drag}} \sin\theta_h E_L \Bigg) (E_L \sin\theta_h)^{-1}.\end{aligned} \tag{12}$$

The adhesive pressure of glycoproteins (P) can be expressed as the force exerted within the bound area, and can be represented as follows [41]:

$$P = \frac{\left(F_n + \frac{m_e g}{n_G}\right) n_G \Delta E_L^2}{2\theta_h E_R \Delta E_L},$$

where n_G is the concentration of glycoproteins required for the minimum attachment area. Inserting P into Eq. (12) will result in:

$$\begin{aligned}\mathbf{T} = \Bigg(& \mathbf{W_{dl}} l_1 + \mathbf{W_h}\left(\frac{E_L}{2} - \frac{\Delta E_L}{2} + l_1\right)\cos\theta_h \\ & + \frac{\left(F_n + \frac{m_e g}{n_G}\right) n_G \Delta E_L}{2\theta_h E_R} + \mathbf{F_{Drag}} \sin\theta_h E_L \Bigg) (E_L \sin\theta_h)^{-1}.\end{aligned} \tag{13}$$

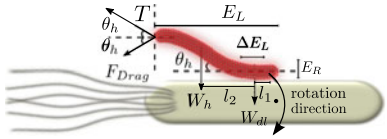

Fig. 7. The force model of an Ebola virus on the bacterium going through a tumbling process. This illustration shows the forces acting on the angular binding for the Ebola virus. The angular binding only happens on locations of turns when the Ebola virus is being pulled outwards during the tumbling process.

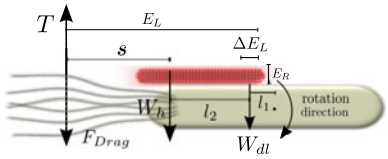

Fig. 8. The force model of the Ebola virus on the bacterium going through a tumbling process. This illustration shows the forces acting on the flat binding for the Ebola virus. The flat binding only occurs on locations of turns when the Ebola virus is being pushed up against the bacterium during the tumbling process.

4.4 Tension Force for Tumbling Motion

When a bacterium tumbles, depending on the position of the Ebola virus binding point, there will be two different types of force models, namely, *angular* and *flat* binding. Fig. 6 illustrates these binding points on the bacterium. As the bacterium rotates at the centre point of the body, the angular binding will occur when the Ebola virus encounters a pulling force (e.g., at the front of the bacterium when it tumbles clockwise), while the flat binding occurs at the tail end of the body when the virus is pushed through the circular motion. Fig. 7 illustrates the force model for the angular binding, while the flat binding model is illustrated in Fig. 8.

4.4.1 *Angular Binding*

Since the motion is a continuous rotational spin at a fixed point, the sum of the momentum is represented as follows:

$$\sum M = I\alpha, \tag{14}$$

where I is the inertial momentum of the bacterium as well as the Ebola virus, and α is the angular acceleration during the tumbling process, which is represented as:

$$\begin{aligned}\alpha &= \frac{d\omega}{dt} \\ &= \frac{2\pi f_t}{\lambda_{Tumble}},\end{aligned}$$

where f_t is the frequency of tumbling. Therefore, the inertial momentum is represented as:

$$I = \frac{m_B L^2}{12} + m_e\left(E_{hl}\cos\theta_h + \frac{\Delta E_L}{2} + l_1\right), \tag{15}$$

where E_{hl} is the length of the virus that is hanging, m_B is the mass and L is the half length of the bacterium. For the angular binding, considering Eq. (14) and (15), Eq. (11) can be represented as:

TABLE 1
Parameters Used to Evaluate the Receptor Binding Force, Tensions, and Drag Force Applied on the Bacterium As Well As the Ebola Virus

Variable	Value	References
E_R	47×10^{-9} m	[22], [23]
E_L	970×10^{-9} m	[22], [23]
B_R	0.5×10^{-6} m	[42]
B_L	1×10^{-6} m	[42]
v_b	20×10^{-6} m/s	[42]
m_e	5.45×10^{-19} kg	[22], [23]
m_b	1×10^{-18} kg	[42]
$[B_0]$	6.7×10^{-6} proteins/μm^2	*
$[V_0]$	2.8×10^{-2} proteins/μm^2	*
f_t	1.37 tumbles/s	[43]
ϕ	from $\pi/100$ rad to $\pi/10$ rad	*
T_a	310 K	*
k_B	0.00831446211 kJ/mol/K	**
ρ_{blood}	1060 kg.m^{-33}	[38]
g	9.8 m/s^2	**
μ_s	3×10^{-3} Pa.s	**
D_v	5 cm	*

** Refers to values chosen by the authors. ** Refers to standard values.*

$$I\alpha = \mathbf{W_{dl}} l_1 + \mathbf{W_h}\left(\frac{E_L}{2} - \frac{\Delta E_L}{2} + l_1\right)\cos\theta_h + \frac{\left(F_n + \frac{m_e g}{n_G}\right) n_G \Delta E_L}{2\theta_h E_R} + \mathbf{F_{Drag}} \sin\theta_h E_L - T E_L \sin\theta_h,$$

and from the perspective of the tension **T**, this is represented as:

$$\mathbf{T} = \left(\mathbf{W_{dl}} l_1 + \mathbf{W_h}\left(\frac{E_L}{2} - \frac{\Delta E_L}{2} + l_1\right)\cos\theta_h + \frac{\left(F_n + \frac{m_e g}{n_G}\right) n_G \Delta E_L}{2\theta_h E_R} + \mathbf{F_{Drag}} \sin\theta_h E_L - \frac{m_B L^2}{12} - m_e\left(E_{hl}\cos\theta_h - \frac{\Delta E_L}{2} - l_1\right)\alpha\right) * (E_L \sin\theta_h)^{-1}. \quad (16)$$

4.4.2 Flat Binding

For the flat binding during the tumbling process, Eq. (16) can be simplified because there is no angle of attachment between the Ebola virus and the bacterium. This means that a large part of the virus will lie flat on the bacterium during rotation. This scenario is presented in Fig. 8. In this case, the tension **T** is represented as:

$$\mathbf{T} = \left(\mathbf{W_{dl}} l_1 + \mathbf{W_h}\left(\frac{E_L}{2} - \frac{\Delta E_L}{2} + l_1\right) + \frac{\left(F_n + \frac{m_e g}{n_G}\right) n_G \Delta E_L}{2\theta_h E_R} + \mathbf{F_{Drag}} E_L - \left(\frac{m_B L^2}{12} - m_e\left(E_{hl} - \frac{\Delta E_L}{2} - l_1\right)\right)\alpha\right)(E_L)^{-1}. \quad (17)$$

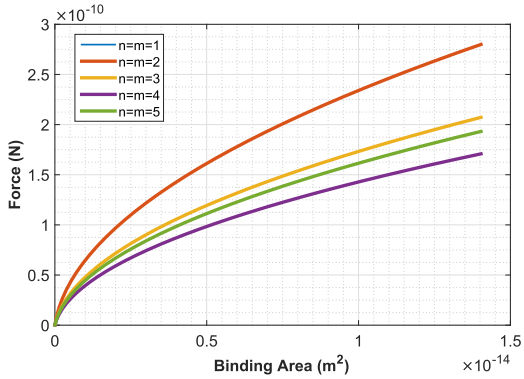

Fig. 9. Analysis of receptor binding force for five different valency configurations.

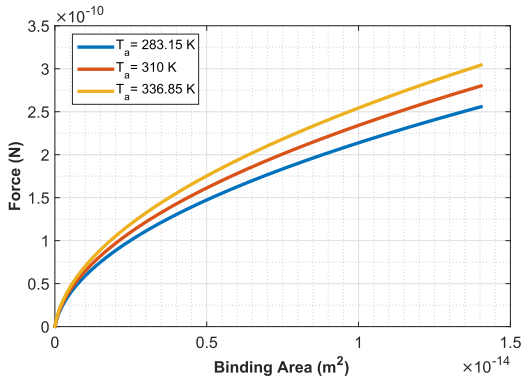

Fig. 10. Analysis of receptor binding force for two different temperatures. The temperature difference considered in this analysis (normal body temperature vs fever) was not sufficient to produce significant changes in the attachment force.

5 Analysis and Simulations

First, we will present the analysis of the binding forces and tensions for the virus attachment to an individual bacterium. This will then be followed by simulations that will evaluate the microfluidic attenuator performance of the Ebola collection process. The values for all the parameters used in the binding force analysis and simulations are presented in Table 1.

5.1 Binding Force and Tensions Analysis

The aim of the analysis is to evaluate the effect of tension forces acting on the attachment point between the Ebola virus and the bacterium, and how this impacts on the protein binding force. The binding force analysis is presented in Figs. 9 and 10, while the opposing forces analysis is presented in Figs. 11, 12 and 13.

The binding force relies on the bacterial and viral proteins valency, and its models were presented in Eq. (2), (3), (4), (5), (6). Therefore, we considered different fixed values of n and m to evaluate their impact on the resulting binding force (see Fig. 9). Even if the number of bonds increases, the ratio n/m will still remain the same. For $n = \{1, 2\}$ and $m = \{1, 2\}$, the binding force was almost the same with less than 1 percent difference, and this was the highest value achieved. The chosen protein, TIM-1, can bind to two or three proteins at same time (i. e. $1 \leq m \leq 3$) and, as presented in Fig. 9, this resulted in the highest binding force values for all possible attachment areas, which also reflects

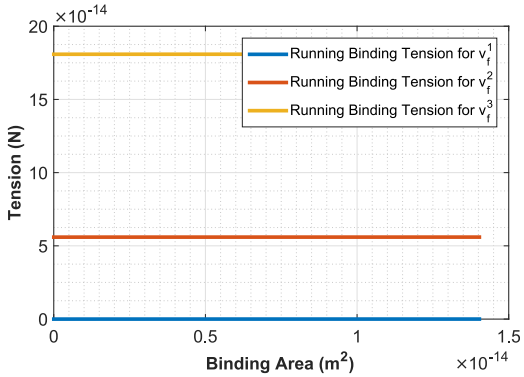

Fig. 11. Analysis of the effect of three different blood velocities on the tension exerted onto the attachment area. We evaluated the opposing forces for $v_f^1 = 0\ \mu$m/s, $v_f^2 = 10\ \mu$m/s, and $v_f^3 = 20\ \mu$m/s.

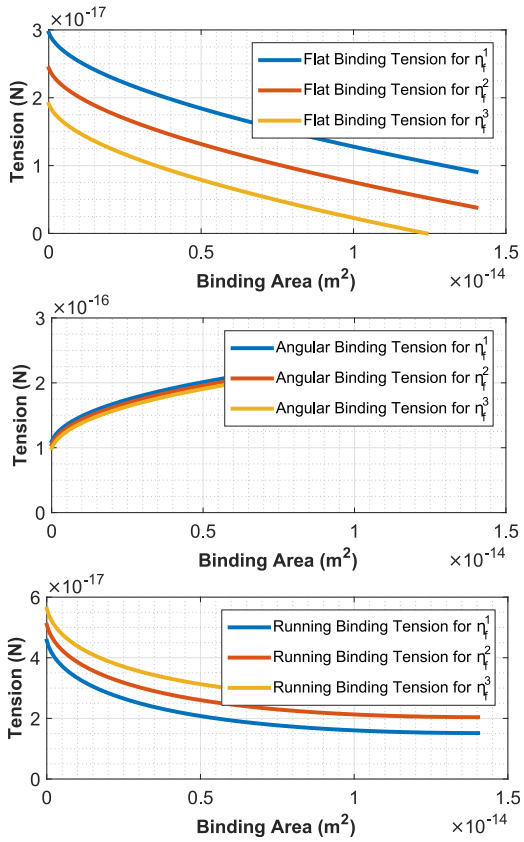

Fig. 12. Analysis of the effect of three different blood viscosities on the tension exerted onto the attachment area. We evaluated the opposing forces for $\eta_f^1 = 3 \times 10^{-3}$ Pa · s, $\eta_f^2 = 4 \times 10^{-3}$ Pa · s, and $\eta_f^3 = 5 \times 10^{-3}$ Pa · s.

the most suitable protein configuration. In Fig. 10, we analysed the effect of temperature on the binding force. We considered three different temperatures to observe different behaviours that can arise. Normal human body temperature is 309.65 K and during fever this is elevated to 313 K. The latter value is also the average temperature of countries where the disease outbreak occurred. As we can observe, the temperature does not produce significant changes in the receptor binding force behaviour, even for high temperatures such as $T_a = 336.85$ K.

The opposing forces acting on the attachment area can be increased or lowered depending on variations for a number of parameters: blood velocity, blood viscosity and angle of attachment between the Ebola virus and the bacterium.

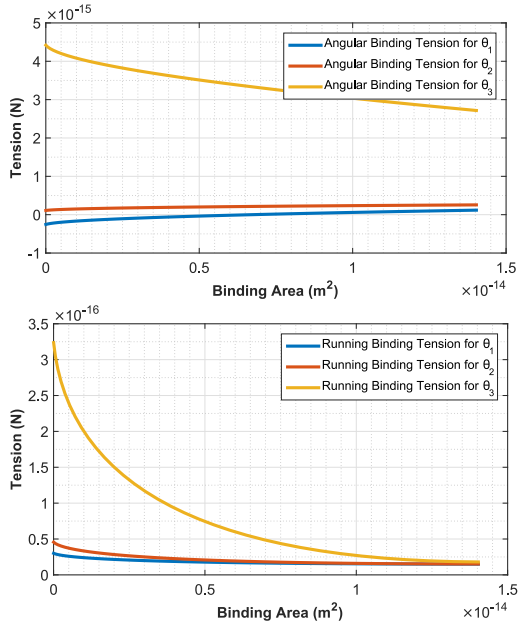

Fig. 13. Analysis of the angular and running binding tensions. Three different attachment angles were considered in this analysis: $\theta_1 = 10$ rad, $\theta_2 = 5$ rad, and $\theta_3 = 0.5$ rad

When the blood enters the microfluidic chamber, it will gain a certain velocity that could be high enough to increase the tension on the attachment point which could lead to breakage. In Fig. 11 we considered three different velocities (v_f^1, v_f^2 and v_f^3) and evaluated their impact on the binding force when the bacterium is running in a straight line (worst case scenario). As the velocity increases, we can observe that the tension increases as well. However, if the blood velocity is much higher than the bacteria velocity, this can become an issue. In this case, when the blood flows into the chamber, it will disrupt the bacteria movement by pushing them toward the opposite border of the compartment. To avoid this effect, the bacteria need to be placed inside the microfluidic chamber when the blood is at rest, and removed before the blood is pumped back into the body.

The patient blood can be more or less viscous depending on the health condition. Different viscosity values can produce significant changes on the drag force that could result in higher tension on the attachment point between the virus and the bacterium. Fig. 12 shows the effect of three different viscosity values on the tension applied on B_{Area}. Higher viscous blood will have a larger impact when the bacteria are moving, while a less viscous blood will affect the tension when the bacteria is tumbling. For all cases presented in Fig. 12, the changes to the tension on the attachment point are reasonably low. This result demonstrates that the blood viscosity will not impact the proposed attenuator system performance. The same occurs if we change the attachment angle, as shown for both the running and angular binding analysis (Fig. 13). For this analysis, we considered three different attachment angles between the Ebola virus and the bacterium. As we can observe from the plots, when the angle increases, the tension applied to detach the virus from the bacterium decreases. Furthermore, for $\theta \geq 5$ rad, the angular binding tension enhances the attachment rather than opposing to detach the virus.

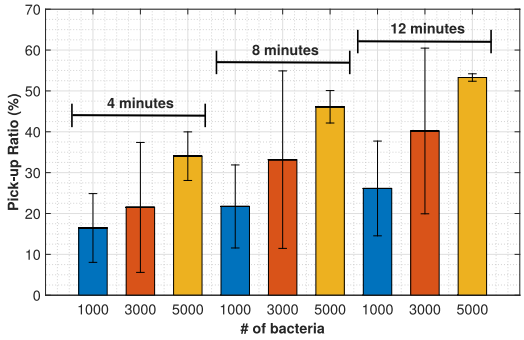

Fig. 14. The pickup ratio increased proportionally with respect to the different simuation times. For 4 minutes, more than 30 percent of the available virus were captured; for 8 minutes, more than 40 percent; and for 12 minutes, more than 50 percent.

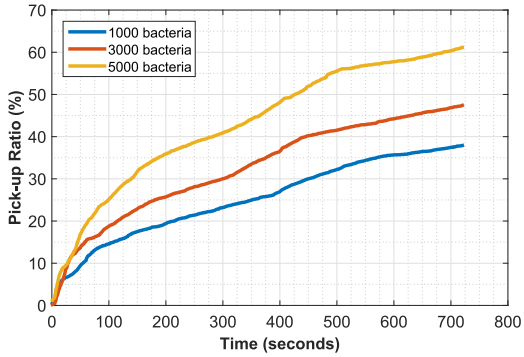

Fig. 15. The quantity of the Ebola virus that are captured with respect to time for different quantities of bacteria. The area considered is 5x5 cm.

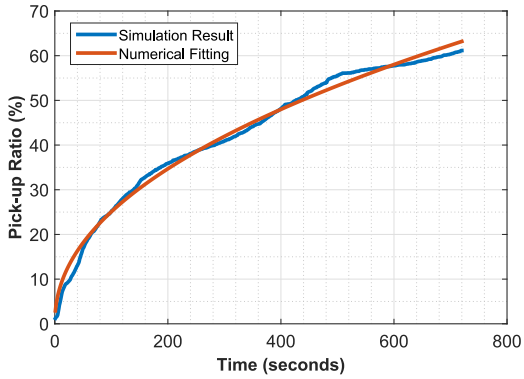

Fig. 16. The filter function $f_b(t)$ was numerically evaluated for 5,000 bacteria. This function can be used to predict the time needed to reach the desired pick-up ratio.

5.2 Microfluidic Attenuator Trapping Simulations

In order to validate the Ebola virus trapping process by the bacteria, we conducted several simulations for the different environments that the system could be exposed. We are interested in evaluating the attenuator model performance for the initial stage of the infection, where the number of Ebola is approximately 10^4 virus (per ml of blood) [44]. For all considered scenarios, the Ebola virus were randomly distributed in a microfluidic chamber square area with a size of 25 cm^2, while the bacteria are placed in an external compartment.

After been released into the chamber, from the compartment ($x = 0$ and along the y-axis, the bacteria swim to capture the Ebola virus. In our scenario, the number of Ebola virus is higher than the number of bacteria. To ensure a constant blood viscosity value (3×10^{-3} $\mathrm{Pa \cdot s}$), the simulation duration was limited by the amount of time before clotting naturally occurs, which is between 8 and 15 minutes [45]. We also considered a static blood flow ($v_f = 0$), small attachment angle ($\theta \leq 0.5$ rad), and the binding force was generated by a trivalent protein interaction ($n = m = 3$).

Based on the analysis presented in Section 5.1, we found that the attachment area has an important effect on the reliability of the binding process. The area limit defined in Eq. (7) is used to determine the maximum number of virus that can attach to each bacterium (this is calculated by considering the bacteria shape as a cylinder, and determining the area of each virus that binds to the surface membrane). In our simulations, for each contact between a bacterium and a virus we evaluate Eq. (7). If the bacterium area is already full of virus, or if the attachment area is larger than the area available, this means that there is no remaining space on the bacterium surface. The results presented in Figs. 9, 10 and angular binding tension in Fig. 12 showed that an increase of B_{Area} resulted in a larger binding force or opposing tensions. At the same time, the results presented in Figs. 11, 12 (running and flat binding tensions) and 13 showed an inverse relationship with B_{Area}. Therefore, in order to simulate a realistic scenario, we consider various random attachment areas between the Ebola virus and the bacteria.

The pick-up ratio was evaluated for different Ebola densities, simulation times, and quantity of bacteria. Fig. 14 presents the performance of the attenuator, which is the ratio of the average number of Ebola virus captured (10^4, 5×10^4 and 10^5 virus) by 1000, 3000 and 5000 bacteria within 4, 8 and 12 minutes. As we can see from the results, the quantity of virus is reduced with respect to the number of bacteria and duration allowed for the collection process.

Since each bacterium will have an attachment limit in terms of bound Ebola virus, after a certain amount of time the system is expected to became saturated. The next set of experiments is designed to measure the time required before saturation occurs. The number of Ebola virus were fixed at 10,000 and three quantities of bacteria were considered (1000, 3000, 5000), while the simulation time was fixed at a maximum of 720 seconds, and the simulations were run for 10 times and averaged. The time, 720 seconds, is selectedto avoid blood clotting. Fig. 15 presents the average pick-up ratio, where after 720 seconds 1000 bacteria achieved 37.89 ± 12.6 percent of the total number of virus, 3000 bacteria achieved 47.41 ± 24.76 percent and 5000 bacteria achieved 61.15 ± 13.56 percent. We can also observe in Fig. 15 that the bacteria do not achieve their saturation point within the considered period of 720 seconds. The considered number of Ebola (and their random placement) combined with the random nature of the bacterial swimming process produce the high variance observed, and limits the bacteria from reaching their saturation point within 720 seconds. We previously defined the model for the attenuator in Eq. (1), which also includes the attenuator function $f_b(t)$ that determines the amount of Ebola virus to be picked up as a function of the time. This function can be estimated from the saturation experiments. As an example, considering that 5000 bacteria achieved the highest pick-up ratio, we used this result to evaluate numerically the attenuator function $f_b(t)$ for 10,000 virus, and predict the time

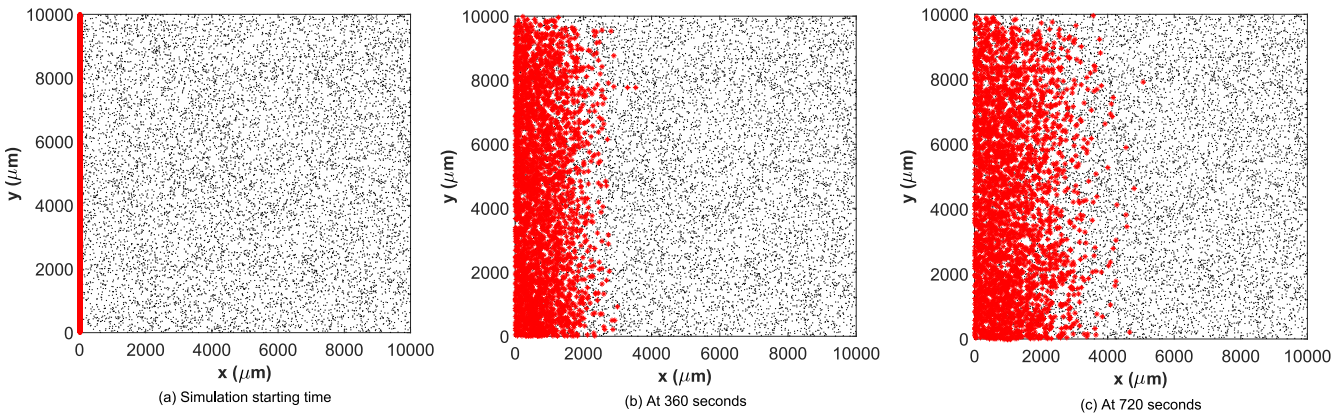

Fig. 17. The placement of bacteria have an impact on the spatial distribution of the virus. (a) At the start of the simulation, the bacteria where placed along the *y*-axis ($x = 0$) and the virus is randomly distributed within the chamber. (b) At 360 seconds, bacteria could filter a small portion of the area. (c) At 720 seconds, bacteria mobilized to more than 30 percent of the chamber's length.

required to reach the desired pick-up ratio (see Fig. 16), and this is represented as:

$$f_b(t) = 2.903t^{0.4682}. \tag{18}$$

The pick-up process can also be observed spatially. In Fig. 17, 10,000 Ebola virus were spread randomly within the chamber (with an area of $1\ \mathrm{cm}^2$) and 3,000 bacteria were released along the *y*-axis ($x = 0$). Within 720 seconds, the number of bacteria reached approximately 5,000 μm. This also demonstates the time taken by the bacteria to move within the area and perform the Ebola pick-up. It can be also observed from Fig. 17 that the bacteria is able to only cover a small portion of the area. This result suggests that a proper chamber design is important to optmise the pick-up process. The chamber geometry will depend on the concentration of the virus for the desired blood volume and the number of bacteria used to collect them. This is still a open problem that should be addressed during the attenuator design.

6 Conclusion

The emergence of Ebola virus in recent years has motivated the need for effective treatment solutions to curb the spreading process. In this paper, we presented an approach where bacteria, genetically engineered, are capable of trapping Ebola virus that bind on its surface. The approach requires blood to be temporarily transported through an external tube that is connected through a microfluidic chamber containing the engineered bacteria. Our approach includes the engineering of receptors on the surface of the bacteria that are compatible to the glycoproteins found on the membrane of the Ebola virus. Our analysis found that the binding process of the Ebola virus on the bacteria is highly dependent on the valency of both viral and bacterial proteins, as well as the attachment area. The paper also presented a simulation model of the bacteria hunting process of the Ebola virus within a confined area. The analysis includes the saturation time of the Ebola virus collection process, as well as the collection and trapping performance when the number of bacteria and Ebola virus varies. Our results show that for the considered simulation time, the bacteria can collect the virus without reaching its attachment limit, and the performance of the Ebola virus trapping quantity is highly dependent on the number of bacteria that are deployed. Although this paper only concentrated on the *E.coli* bacteria, the approach can also extend to other attenuated strains of bacteria such as *Salmonella* [46], and also to other virus that can bind to TIM-1. The proposed technique also shows the potential of using synthetic biology to build a biomedical machinery to clean human blood from virus.

Acknowledgments

This work was supported by the CIRCLE Project (grant no. 665564) and partially funded by 1) Science Foundation Ireland via the CONNECT Research Centre (grant no. 13/RC/2077), 2) via the FiDiPro program of the Academy of Finland (Nano communication Networks), 2012-2016, 3) the Academy of Finland Research Fellow grant (no. 284531), and 4) the US National Science Foundation through grant MCB-1449014.

References

[1] K. A. Alexander, et al., "What factors might have led to the emergence of Ebola in West Africa?" *PLoS Neglected Tropical Diseases*, vol. 9, no. 6, Jun. 2015, Art. no. e0003652.
[2] P. E. Kilgore, et al., "Treatment of Ebola Virus disease," *Pharmacotherapy*, vol. 35, no. 1, pp. 43–53, Jan. 2015
[3] World Health Organization (WHO) FAQ, "Ebola vaccines, therapies, and diagnostics". 2015. [Online]. Available: http://www.who.int/medicines/emp_ebola_q_as/en/, 2015.
[4] M. Shuchman, "Ebola vaccine trial in west Africa faces criticism," *Lancet*, vol. 385, no. 9981, pp. 1933–1934, May 2015.
[5] M. V. Herp, et al., "Favipiravir-a prophylactic treatment for Ebola contacts?" *Lancet*, vol. 385 no. 9985, Jun. 2015, Art. no. 2350.
[6] R. Breitling and E. Takano, "Synthetic biology advances for pharmaceutical production," *Current Opinion Biotechnology*, vol. 35, pp. 46–51, Mar. 2015.
[7] G. Gehring, et al. "The clinically approved drugs amiodarone, dronedarone and verapamil inhibit filovirus cell entry," *J. Antimicrobial Chemotherapy Adv. Access*, vol. 69, no. 8, pp. 2123–2131, Aug. 2014.
[8] J. M. Dye, et al., "Postexposure antibody prophylaxis protects nonhuman primates from filovirus disease," *Proc. Nat. Acad. Sci. United States America*, vol. 109 no. 13, pp. 5034–5039. Mar. 2012.
[9] X. Qiu, et al. "Reversion of advanced Ebola virus disease in nonhuman primates with ZMapp," *Nature*, vol. 514, no. 7520, pp. 47–53, Oct. 2014.
[10] J. Misasi, et al., "Structural and molecular basis for Ebola virus neutralization by protective human antibodies," *Sci.*, Feb. 2016.
[11] D. Corti, et al., "Protective monotherapy against lethal Ebola virus infection by a potently neutralizing antibody," *Sci.*, Feb. 2016.
[12] J. Kouznetsova, et al., "Identification of 53 compounds that block Ebola virus-like particle entry via a repurposing screen of approved drugs," *Emerging Microbes Infections*, vol. 3, no. 12, 2014, Art. e84.

[13] A. R. Oany, et al., "Highly conserved regions in Ebola virus RNA dependent RNA polymerase may be act as a universal novel peptide vaccine target: A computational approach," *Silico Pharmacology*, vol. 3, no. 7, 2015.
[14] T. Nakano, et al., "Molecular communication among biological nanomachines: A layered architecture and research issues," *IEEE Trans. NanoBioscience*, vol. 13, no. 3, pp. 169–197, Sep. 2014.
[15] D. P. Martins, et al., "Using competing bacterial communication to disassemble biofilms," in *Proc. 3rd ACM Int. Conf. Nanoscale Comput. Commun.*, Sep. 2016, Art. no. 18.
[16] C. Piñero-Lambea, et al., "Engineered bacteria as therapeutic agents," *Current Opinion Biotechnology*, vol. 35, pp. 94–102, Jun. 2015.
[17] L. Vangelista, et al., "Engineering of Lactobacillus jensenii to secrete RANTES and a CCR5 antagonist analogue as live HIV-1 blockers," *Antimicrobial Agents Chemotherapy*, vol. 54, no. 7, pp. 994–3001, Jul. 2010.
[18] P. E. Massa, et al., "Salmonella engineered to express CD20-targeting antibodies and a drug-converting enzyme can eradicate human lymphomas," *Blood*, vol. 122, no. 5, pp. 705–714, Aug. 2013.
[19] D. R. Asher, et al., "The erythrocyte viral trap: Transgenic expression of viral receptor on erythrocytes attenuates coxsackievirus B infection," in *Proc. Nat. Acad. Sci. United States America*, vol. 102, no. 36, Sep. 2005.
[20] J. J. Dennehy, et al., "Virus population extinction via ecological traps," *Ecology Lett.*, vol. 10, no. 3, pp. 230–240, Mar. 2007.
[21] M. Mammen, et al., "Polyvalent interactions in biological systems: Implications for design and use of multivalent ligands and inhibitors," *Angewandte Chemie Int. Edition*, vol. 37, no. 20, pp. 2754–2794, Nov. 1998.
[22] A. M. King, et al., *Virus Taxonomy: Ninth Report of the International Committee on Taxonomy of Viruses*. Amsterdam, The Netherlands: Elsevier, 2012.
[23] P. Ascenzi, et al., "Ebolavirus and Marburgvirus: Insight the Filoviridae family," *Molecular Aspects Med.*, vol. 29, no. 3 pp. 151–185, Jun. 2008.
[24] A. C. Zampieri, et al., "Immunopathology of highly virulent pathogens: Insights from Ebola virus," *Nature Immunology*, vol. 8, no. 11, pp. 1159–1164, Nov. 2007.
[25] M. Bray, "Pathogenesis of viral hemorrhagic fever," *Current opinion in immunology*, vol. 17, no. 4, pp. 399–403, Mar. 2005.
[26] N. Sullivan, et al., "Ebola Virus pathogenesis: Implications for vaccines and therapies," *J. Virology*, vol. 77, no. 18, pp. 9733–9737, Sep. 2003.
[27] E. H. Miller and K. Chandran, "Filovirus entry into cells - new insights," *Current Opinion Virology*, vol. 2, no. 2, pp. 206–214, Apr. 2012.
[28] M. Mazzon and J. Mercer, "Lipid interactions during virus entry and infection," *Cellular Microbiology*, vol. 16, no. 10, pp. 1493–1502, Oct. 2014.
[29] E. Rothenberg, et al., "Single-virus tracking reveals a spatial receptor-dependent search mechanism," *Biophysical J.*, vol. 100, no. 12, pp. 2875–2882, Jun. 2011.
[30] Z. Chen, et al., "Interactions of human T cell immunoglobin mucins with apoptotic cells," *J. Huazhong Univ. Sci. Technol.*, vol. 32, no. 1, pp. 9–16, Feb. 2012.
[31] C. Dressaire, et al., "BolA is a transcriptional switch that turns off motility and turns on biofilm development," *MBio*, vol. 6, no. 1, pp. 1–13, 2015.
[32] X. Liu and T. Ferenci, "Regulation of porin-mediated outer membrane permeability by nutrient limitation in Escherichia coli," *J. Bacteriology*, vol. 180, no. 15, pp. 3917–3922, 1998.
[33] M. Morita, et al., "Characterization of a virulent bacteriophage specific for Escherichia coli O157:H7 and analysis of its cellular receptor and two tail fiber genes," *FEMS Microbiology Lett.*, vol. 211, no. 1, pp. 77–83, 2002.
[34] K. Hantke and V. Braun, "Functional interaction of the tonA/tonB receptor system in Escherichia coli," *J. Bacteriology*, vol. 135, no. 1, pp. 190–197, 1978.
[35] S. X. Sun, and D. Wirtz, "Mechanics of enveloped virus entry into host cells," *Biophysical J.*, vol. 90, no. 1, pp. 10–12, Jan. 2006.
[36] V. A. Petrenko and V. J. Vodyanoy, "Phage display for detection of biological threat agents," *J. Microbiological Methods*, vol. 53, no. 2, pp. 253–262, 2003.
[37] V. M. Krishnamurthy, et al., "Multivalency in Ligand design," *Fragment-Based Approaches Drug Discovery*, vol. 34, pp. 11–53, 2006.
[38] L. Arcese, et al., "Dynamic behavior investigation for trajectory control of microrobot in blood vessels," in *Proc. IEEE/RSJ Int. Conf. Intell. Robots Syst*, Oct. 2010, pp. 5774–5779.
[39] R. M. Harshey, "Bacterial motility on a surface: Many ways to a common goal," *Annu. Rev. Microbiology*, vol. 57, no. 1, pp. 249–273, 2003.
[40] Z. Wang, et al., "Validating models of bacterial Chemotaxis by simulating the random motility coefficient," *Proc. 8th IEEE Int. Conf. BioInform. BioEng.*, 2008, pp. 1–5.
[41] M. P. Reyes and R. S. Fearing, "Macromodel for the mechanics of Gecko Hair Adhesion," in *Proc. IEEE Int. Conf. Robot. Automation*, 2008, pp. 1602–1607.
[42] W. R. Schneider and R. N. Doetsch, "Effect of viscosity on bacterial motility," *J. Bacteriology*, vol. 117, no. 2, pp. 696–701, Feb. 1974.
[43] U. Alon, et al., "Response regulator output in bacterial chemotaxis," *EMBO J.*, vol. 17, no. 15, pp. 4238–4248, Aug. 1998.
[44] M. de La Vega, et al., "Ebola viral load at diagnosis associates with patient outcome and outbreak evolution," *J. Clinical Investigation*, vol. 125, no. 12, pp. 4421–4428, Dec. 2015.
[45] L. Silvestri, *Saunders Comprehensive Review for the NCLEX-RN Examination*. St. Louis, MO, USA: Elsevier, 2014, pp. 116–117.
[46] J. F. Toso, et al., "Phase I study of the intravenous administration of attenuated Salmonella typhimurium to patients with metastatic melanoma," *J. Clinical Oncology*, vol. 20, no. 1, pp. 142–152, Jan. 2002.

Daniel Perez Martins (S'12) received the BSc degree in telecommunications engineering from the University Center Jorge Amado, Unijorge, Brazil, in 2009, and the MSc degree in electrical engineering from the Federal University of Campina Grande, Brazil, in 2013. He is working toward the PhD degree associated with the Telecommunications Software and Systems Group (TSSG) and the Waterford Institute of Technology, Ireland. His interests include bacteria-based nanosystems, synthetic biology, and molecular communication. His experiences concentrates on mathematical modelling of telecommunications systems, signal processing and analysis, computer networks, and molecular communication. He is also a reviewer for the *Nano Communications Networks Journal* and for the *IEEE Internet of Things Journal*. He is a graduate student member of the IEEE and South Ireland Rep of the IEEE UK & Ireland Young Professionals Affinity Group.

Michael Taynnan Barros received the BTech degree in telematics from the Federal Institute of Education, Science and Technology of Paraiba, in 2011, the MSc degree in computer science from the Federal University of Campina Grande, in 2012, and the PhD degree in telecommunication software from the Waterford Institute of Technology, in 2016. He is currently an Irish research council government of Ireland postdoctoral research fellow associated with TSSG, WIT. His research interests include molecular communications, nanonetworks, and 5G technology for connected health. He has published more than 40 research papers in diverse journals such as the *IEEE Transactions on Communications*, the *IEEE Transactions on Nanotechnology*, and conferences in the area of wireless communications, optical communications, ad-hoc networks, as well as molecular and nanoscale communications. He is also a reviewer for many journals and participated as a technical program committee member and reviewer for various international conferences. In 2017, he served as the technical program co-chair for the 3rd International Workshop on Nanoscale Computing and Communications (NsCC) held in conjunction with the NEW2AN conference. Also, he served as the chair of the 5GPPP Network Management, QoS and Security Working Group and the chair of the 2nd Network Management, QoS and Security for 5G Networks held in conjunction with the EuCNC 2017. He is a member of the IEEE.

Massimiliano Pierobon (S'05-M'13) received the MS degree in telecommunication engineering from the Politecnico di Milano, Italy, in 2005, and the PhD degree in electrical and computer engineering from the Georgia Institute of Technology, Atlanta, Georgia, in 2013. Since August 2013, he has been an assistant professor in the Department of Computer Science and Engineering, University of Nebraska-Lincoln (UNL), Nebraska, where he also holds a courtesy appointment in the Department of Biochemistry. His research interest include molecular communication, nanonetworks, synthetic biology, intra-body networks, and the Internet of Bio-Nano Things. He received the BWN Lab Researcher of the Year Award at the Georgia Institute of Technology for his outstanding research achievements in 2011. He was also named IEEE Communications Letters 2013 Exemplary Reviewer in appreciation for his service as a referee, and he is the recipient of the 2016 UNL CSE Upper Level Teaching Award. He is an editor of the *IEEE Transactions on Communications*. He was a guest-editor for special issues for the *IEEE Internet of Things Journal* and the *Nano Communication Networks (Elsevier) Journal*. He was TPC co-chair for ACM NanoCom 2016 and TPC vice-co-chair for ACM NanoCom 2015. He is a faculty mentor for the UNL iGEM team. He is a member of the IEEE.

Meenakshisundaram Kandhavelu received the graduate degree from the American College, Madurai Kamaraj University, India, in 2002, the MSc degree in animal biotechnology from Bharathidasan University, India, in 2005, and the PhD degree in pharmaceutical sciences (research disciplinary, chemical and pharmaceutical sciences and biotechnology) from the University of Camerino, Italy (with the mobility research mobility research work at the University of Milan), in 2008. He was an intern researcher in the stem cell and developmental biology research group, Genomic Institute of Singapore, in 2004-2005. During 2009, he worked as a postdoctoral researcher with the A.I.Virtanean Institute for Molecular Sciences, Finland. Later, in 2010-2012, he continued his post-doctoral research with the Department of Signal Processing. Since 2013, he has been working as a group leader of the Molecular Signaling Lab (MS Lab) and as an assistant professor/adjunct professor with the same department, TUT. His research interest includes molecular signal processing and health informatics. He has authored more than 35 international refereed publication. He has made a contribution to the field of molecular signal processing.

Pietro Lio' is a reader in computational biology with the Computer Laboratory, University of Cambridge. His affiliations also include the Cambridge Computational Biology Institute. His work spans machine learning and computational models for health Big Data, personalised medicine research, multi-scale/multi-omic/multi-physics modelling, and data integration methods, with more than 230 peer reviewed papers. He has edited several books and given more than 20 keynote talks.

Sasitharan Balasubramaniam (SM'14) received the bachelor's degree in electrical and electronic engineering, and the PhD degree both from the University of Queensland, in 1998 and 2005, respectively, and the master's degree in computer and communication engineering from the Queensland University of Technology, in 1999. He is currently a senior research fellow with the Nano Communication Centre, Department of Electronic and Communication Engineering, Tampere University of Technology, Finland. Previously, he was a research fellow with the Telecommunication Software and Systems Group, Waterford Institute of Technology, Ireland, where he worked on a number of Science Foundation Ireland projects. His current research interests include bio-inspired communication networks, as well as molecular communications. He has published more than 70 papers and actively participates in a number of technical programme committee for various conferences. He was the TPC co-chair for ACM NANOCOM 2014 and IEEE MoNaCom 2011, both conferences which he co-founded. He is currently an editor for the *IEEE Internet of Things Journal* and the *Elsevier Nano Communication Networks*. He is a senior member of the IEEE.